Supplementary Information

Cadmium Isotope Variations in the Southern Ocean

Zichen Xue[1], Mark Rehkämper[1*], Tristan J. Horner[2,3], Wafa Abouchami[4,5], Rob Middag[6,7], Tina van de Flierdt[1], and Hein J. W. de Baar[5]

[1] Department of Earth Science and Engineering, Imperial College London, London SW7 2AZ, UK

[2] Department of Earth Sciences, University of Oxford, Oxford OX1 3AN, UK

[3] Department of Marine Chemistry and Geochemistry, Woods Hole Oceanographic Institution, Woods Hole MA 02543, USA

[4] Institut für Mineralogie, WWU Münster, 48149 Münster, Germany

[5] Max Planck Institute for Chemistry, P.O. Box 3060, 55020 Mainz, Germany

[6] Royal Netherlands Institute for Sea Research, P.O. Box 59, 1790 AB Den Burg, The Netherlands

[7] Department of Chemistry, University of Otago, P.O. Box 56, Dunedin 9054, New Zealand

* corresponding author: markrehk@imperial.ac.uk, +44 20 7594 6391

Supplement Section 1

Tables with detailed data for the seawater samples from this study and the study of Abouchami et al. (2011)

Table S1.1. Detailed data for the Zero Meridian Weddell Gyre surface seawater samples of this study

Sampling Station	Date	Latitude	Longitude	Salinity	θ (°C)	$[PO_4^{3-}]$ (µmol/kg)	[Si] (µmol/kg)	$[NO_2^- + NO_3^-]$ (µmol/kg)	$[NO_2^-]$ (µmol/kg)	$[NO_3^-]$ (µmol/kg)	[Si*] (µmol/kg)	[Cd] (nmol/kg)	$\varepsilon^{114/110}Cd$	±2sd
142	27/02/2008	62.23°S	0.00	33.95	0.44	1.69	57.76	23.69	0.16	23.53	34.23	0.270	6.76	0.50
145	28/02/2008	63.25°S	0.00	33.91	0.59	1.61	53.83	23.31	0.16	23.15	30.68	0.257	7.31	0.50
148	29/02/2008	64.21°S	0.01	33.94	0.60	1.60	46.87	22.91	0.15	22.76	24.11	0.247	7.38	0.50
151	29/02/2008	65.24°S	0.00	33.95	-0.24	1.62	62.49	25.35	0.22	25.14	37.36	0.378	5.39	0.50
153A	29/02/2008	66.00°S	0.73	33.85	-0.21	1.61	61.97	25.74	0.23	25.52	36.46	0.373	6.34	0.50
156	07/03/2008	66.52°S	0.01	33.8	-0.76	1.64	59.23	25.45	0.21	25.25	33.99	0.382	5.76	0.50
160	08/03/2008	66.03°S	0.07°W	34.09	-0.41	1.63	58.70	25.68	0.27	25.41	33.29	0.263	7.48	0.68
162	09/03/2008	66.56°S	0.00	33.84	-0.76	1.67	58.26	25.53	0.21	25.32	32.94	0.386	5.66	0.50
164	09/03/2008	67.02°S	0.01°W	33.94	-0.73	1.77	65.49	27.00	0.23	26.77	38.72	0.434	4.75	0.70
166	10/03/2008	67.58°S	0.00	33.93	-0.76	1.84	67.56	27.50	0.25	27.25	40.32	0.461	4.54	0.70
168	10/03/2008	68.29°S	0.00	33.97	-0.74	1.78	62.87	26.68	0.28	26.40	36.47	0.413	4.83	0.71
170	10/03/2008	68.65°S	0.00	33.93	-0.78	1.74	60.58	25.94	0.27	25.67	34.91	0.384	4.99	0.70
172	10/03/2008	68.96°S	0.00	33.92	-1.02	1.75	60.50	25.93	0.27	25.66	34.84	0.390	5.00	0.50

All samples are surface waters that were collected with an IFISH torpedo and pump line system at 2 to 5 m depth.
The Cd concentration and isotope compositions were measured at the Imperial College London MAGIC laboratories. The $\varepsilon^{114/110}Cd$ values are reported relative to NIST SRM 3108 Cd (Abouchami et al., 2012). The uncertainties quoted for $\varepsilon^{114/110}Cd$ are based on the ±2sd uncertainties determined for multiple analyses of matching standard solutions that were analyzed before and after each sample measurement (see main text for details). Additional results were acquired by other researchers involved in the 2008 GEOTRACES expedition ANT XXIV/3 aboard the RV Polarstern using methods described in Middag et al. (2011) and Middag et al. (2012). The [Si*] values were calculated by $[Si^*] = [Si(OH)_4] - [NO_3^-]$ (Sarmiento et al., 2004).

Table S1.2. Detailed data for the seawater samples from the three depth profiles in the Weddell Gyre and Drake Passage that were analyzed in this study

Sampling Station	Date	Latitude	Longitude	Water Depth (m)	Salinity	θ (°C)	$[O_2]$ (µmol/kg)	$[PO_4^{3-}]$ (µmol/kg)	[Si] (µmol/kg)	$[NO_2^- + NO_3^-]$ (µmol/kg)	$[NO_2^-]$ (µmol/kg)	$[NO_3^-]$ (µmol/kg)	[Si*] (µmol/kg)	DIC (µmol/kg)	[Cd] (nmol/kg)	$\varepsilon^{114/110}Cd$	±2sd
198	20/03/08	65.61°S	36.40°W	25	34.16	-1.45	334.38	1.88	73.33	27.85	0.26	27.59	45.74	2196	0.549	4.04	0.63
198	20/03/08	65.61°S	36.40°W	100	34.51	-1.73	291.98	2.11	83.56	30.68	0.09	30.59	52.97	2235	0.719	2.59	0.35
198	20/03/08	65.61°S	36.40°W	200	34.67	0.24	196.24	2.36	112.35	34.19	0.02	34.17	78.18	2269	0.890	1.68	0.39
198	20/03/08	65.61°S	36.40°W	300	34.67	0.23	196.16	2.38	120.64	34.45	0.02	34.43	86.21	2267	0.888	1.35	0.35
198	20/03/08	65.61°S	36.40°W	400	34.68	0.38	191.00	2.39	118.49	34.43	0.02	34.41	84.08	2271	0.882	0.98	0.35
198	20/03/08	65.61°S	36.40°W	500	34.69	0.40	191.38	2.39	121.52	34.40	0.02	34.39	87.14	2274	0.863	2.48	0.23
198	20/03/08	65.61°S	36.40°W	1000	34.68	0.14	207.62	2.36	126.11	33.96	0.02	33.94	92.17	2267	0.815	2.56	0.26
198	20/03/08	65.61°S	36.40°W	2000	34.66	-0.26	225.64	2.31	125.91	33.20	0.02	33.19	92.73	2258	0.788	2.30	0.35
198	20/03/08	65.61°S	36.40°W	3000	34.66	-0.48	236.17	2.28	124.55	32.70	0.02	32.69	91.87	2254	0.776	2.94	0.65
198	20/03/08	65.61°S	36.40°W	4000	34.65	-0.65	243.14	2.28	124.94	32.69	0.02	32.67	92.27	2250	0.762	2.55	0.65
198	20/03/08	65.61°S	36.40°W	4702	34.64	-0.86	250.41	2.27	115.96	32.54	0.02	32.52	83.44	2249	0.754	1.69	0.65
216	26/03/08	63.70°S	50.84°W	25	34.14	-1.85	305.96	2.05	73.04	28.92	0.12	28.80	44.24	2210	0.645	4.65	0.82
216	26/03/08	63.70°S	50.84°W	100	34.43	-1.81	278.14	2.14	76.25	30.80	0.09	30.71	45.54	2231	0.714	3.29	0.81
216	26/03/08	63.70°S	50.84°W	150	34.44	-1.81	275.83	2.14	77.03	30.81	0.03	30.78	46.25	2231	0.739	2.41	0.23
216	26/03/08	63.70°S	50.84°W	200	34.46	-1.48	271.91	2.17	79.17	31.04	0.03	31.01	48.16	2236	0.773	2.01	0.49
216	26/03/08	63.70°S	50.84°W	400	34.65	0.42	211.87	2.26	99.37	32.38	0.02	32.36	67.01	2259	0.795	2.49	0.23
216	26/03/08	63.70°S	50.84°W	500	34.67	0.47	208.51	2.26	104.25	32.40	0.03	32.37	71.88	2260	0.789	1.97	0.35
216	26/03/08	63.70°S	50.84°W	1000	34.68	0.27	211.33	2.29	115.96	32.89	0.02	32.87	83.09	2260	0.783	2.23	0.49
216	26/03/08	63.70°S	50.84°W	1500	34.67	0.03	219.23	2.30	121.81	33.04	0.02	33.02	88.79	2262	0.782	2.49	0.76
216	26/03/08	63.70°S	50.84°W	2000	34.66	-0.29	231.79	2.27	118.89	32.56	0.03	32.53	86.36	2258	0.771	1.93	0.76
216	26/03/08	63.70°S	50.84°W	2450	34.61	-1.26	279.92	2.18	84.43	31.32	0.01	31.31	53.12	2241	0.737	2.99	0.33
249	09/04/08	56.12°S	63.76°W	8.5	33.87	4.56	304.64	1.66	5.23	24.14	0.27	23.87	-18.64	2125	0.400	6.68	0.63
249	09/04/08	56.12°S	63.76°W	25	33.87	4.56	305.13	1.67	5.24	24.34	0.26	24.08	-18.84	2124	0.395	7.02	0.63
249	09/04/08	56.12°S	63.76°W	75	33.88	4.46	310.15	1.70	5.87	24.38	0.27	24.11	-18.24	2126	0.409	6.72	0.63
249	09/04/08	56.12°S	63.76°W	150	33.99	2.89	302.15	1.87	15.21	27.06	0.07	26.99	-11.78	2148	0.649	3.42	0.63
249	09/04/08	56.12°S	63.76°W	250	34.03	2.32	300.80	1.96	20.57	28.28	0.03	28.25	-7.68	2162	0.641	4.01	0.63
249	09/04/08	56.12°S	63.76°W	400	34.16	2.50	254.70	2.11	31.22	30.49	0.02	30.47	0.75	2188	0.703	3.27	0.63
249	09/04/08	56.12°S	63.76°W	750	34.43	2.52	180.40	-	-	-	-	-	-	2033	0.624	4.04	0.63
249	09/04/08	56.12°S	63.76°W	1250	34.64	2.18	163.92	2.30	79.43	33.18	0.02	33.16	46.27	2257	0.807	2.46	0.35
249	09/04/08	56.12°S	63.76°W	1750	34.71	1.79	170.40	2.24	93.43	32.26	0.01	32.25	61.18	2263	0.761	2.81	0.58
249	09/04/08	56.12°S	63.76°W	2500	34.73	1.30	186.88	2.21	104.12	31.91	0.02	31.89	72.23	2261	0.744	2.40	0.58
249	09/04/08	56.12°S	63.76°W	3000	34.72	0.89	195.36	2.22	115.20	32.14	0.02	32.12	83.08	2261	0.759	2.71	0.58
249	09/04/08	56.12°S	63.76°W	4000	34.69	0.36	210.89	2.24	120.37	32.47	0.03	32.44	87.93	2261	0.763	2.50	0.58
249	09/04/08	56.12°S	63.76°W	4253	34.69	0.35	211.56	2.25	116.98	32.44	0.03	32.41	84.57	2262	0.767	2.83	0.58
202	21/03/08	64.95°S	41.67°W	400	34.68	0.34	194.25	2.38	118.01	34.35	0.04	34.31	83.70	2274	0.892	3.23	0.16
245	08/04/08	56.88°S	62.52°W	2–5	-	-	-	-	-	-	-	-	-	-	0.374	6.81	0.82

θ = Potential temperature. The DIC data for Station 198 and 216 are for samples from a different cast at the same station but taken at the same depth. The Cd concentration and isotope compositions were measured at the Imperial College London MAGIC laboratories. The $\varepsilon^{114/110}Cd$ values are reported relative to NIST SRM 3108 Cd (Abouchami et al., 2012). The uncertainties quoted for $\varepsilon^{114/110}Cd$ are based on the ±2sd uncertainties determined for multiple analyses of matching standard solutions that were analyzed before and after each sample measurement (see main text for details). Additional results were acquired by other researchers involved in the 2008 GEOTRACES expedition ANT XXIV/3 aboard the RV Polarstern using methods described in Middag et al. (2011) and Middag et al. (2012). The [Si*] values were calculated by $[Si^*] = [Si(OH)_4] - [NO_3^-]$ (Sarmiento et al., 2004).

Table S1.3. Sample locations, Cd concentrations and Cd isotope compositions of the Zero Meridian surface seawater samples that were analyzed by Abouchami et al. (2011).

Sampling Station	Region	Sampling Date	Water Depth (m)	Latitude	Longitude	Cd (nmol/kg)	$\varepsilon^{112/110}Cd$	±2sd	$\varepsilon^{114/110}Cd$	±2sd
PS71-101-2	SAZ	13/2/08	10	42.34°S	8.99°W	0.036	3.32	1.12	6.58	2.22
PS71-103-1	ACC	16/2/08	10	46.00°S	5.88°W	0.155	4.96	0.32	9.83	0.63
PS71-104-2	PFZ	16/2/08	14.5	47.67°S	4.29°W	0.260	3.98	0.20	7.89	0.40
PS71-104-2[a]						0.255	3.88	0.41	7.69	0.81
PS71-105	PFZ	17/2/08	2–5	48.04°S	3.82°W	0.249	4.43	0.20	8.78	0.40
PS71-107-3	PFZ	18/2/08	10	50.26°S	1.43°W	0.388	3.16	0.22	6.27	0.44
PS71-109	PFZ	19/2/08	2–5	51.66°S	0.00	0.415	3.00	0.19	5.95	0.38
PS71-111	AAZ	19/2/08	2–5	52.17°S	0.53°E	0.513	2.64	0.11	5.23	0.22
PS71-113-1	AAZ	20/2/08	9.9	53.00°S	0.01°W	0.554	2.51	0.25	4.98	0.50
PS71-114	AAZ	20/2/08	2–5	53.18°S	0.00	0.527	2.51	0.12	4.98	0.24
PS71-117	AAZ	21/2/08	2–5	54.32°S	0.02°W	0.620	2.19	0.15	4.34	0.30
PS71-120	SB-ACC	21/2/08	0	55.23°S	0.00	0.525	2.37	0.14	4.70	0.28
PS71-123	WG	22/2/08	2–5	56.30°S	0.00	0.509	2.20	0.12	4.36	0.24
PS71-126	WG	23/2/08	2–5	57.21°S	0.00	0.525	2.09	0.12	4.14	0.24
PS71-129	WG	24/2/08	2–5	58.20°S	0.00	0.459	2.35	0.14	4.66	0.28
PS71-133	WG	24/2/08	2–5	59.00°S	0.00	0.431	2.38	0.16	4.72	0.32
PS71-136	WG	26/2/08	2–5	60.24°S	0.00	0.392	2.47	0.12	4.90	0.24
PS71-138-1	WG	26/2/08	24.8	61.00°S	0.01°E	0.334	3.32	0.27	6.58	0.54
PS71-139	WG	26/2/08	2–5	61.15°S	0.00	0.314	2.62	0.22	5.19	0.44
PS71-163-1	WG	9/3/08	8.8	67.00°S	0.00	0.460	2.95	0.16	5.85	0.32

The $\varepsilon^{112/110}Cd$ data and ±2sd uncertainties of Abouchami et al. (2011) were corrected to the $\varepsilon^{114/110}Cd$ values used here, based on the simplified conversion of $\varepsilon^{114/110}Cd = \varepsilon^{112/110}Cd \times \beta$, with $\beta = \ln(m114/m110)/\ln(m114/m110)$, where m11X denotes the exact atomic masses of ^{110}Cd to ^{114}Cd (Rehkämper et al., 2011). All εCd values are reported relative to NIST SRM 3108 Cd (Abouchami et al., 2012). Based on a reevaluation of cruise data, the APF is now thought to be located somewhere between PS71-109 and PS71-111. As a consequence, Station PS71-109 is here assigned to the PFZ (rather than the AAZ, as in Abouchami et al., 2011).
SAZ = Subantarctic Zone, ACC = Antarctic Circumpolar Current, PFZ = Polar Frontal Zone, AAZ = Antarctic Zone, SB-ACC = Southern boundary of the ACC, WG = Weddell Gyre.
[a] Duplicate laboratory analysis of the same sample aliquot.

References

Abouchami, W., Galer, S.J.G., de Baar, H.J.W., Alderkamp, A.C., Middag, R., Laan, P., Feldmann, H., Andreae, M.O., 2011. Modulation of the Southern Ocean cadmium isotope signature by ocean circulation and primary productivity. Earth Planet. Sci. Lett. 305, 83-91.

Abouchami, W., Galer, S.J.G., Horner, T.J., Rehkämper, M., Wombacher, F., Xue, Z., Lambelet, M., Gault-Ringold, M., Stirling, C.H., Schonbächler, M., Shiel, A.E., Weis, D., Holdship, P.F., 2012. A common reference material for cadmium isotope studies – NIST SRM 3108. Geostand. Geoanal. Res 37, 5-17.

Middag, R., de Baar, H.J.W., Laan, P., Cai, P.H., van Ooijen, J.C., 2011. Dissolved manganese in the Atlantic sector of the Southern Ocean. Deep-Sea Res. II 58, 2661-2677.

Middag, R., de Baar, H.J.W., Laan, P., Huhn, O., 2012. The effects of continental margins and water mass circulation on the distribution of dissolved aluminum and manganese in Drake Passage. J. Geophys. Res. C01019, doi:10.1029/2011JC007434.

Rehkämper, M., Wombacher, F., Horner, T.J., Xue, Z., 2011. Natural and anthropogenic cadmium isotope variations, in: Baskaran, M. (Ed.), Handbook of Environmental Isotope Geochemistry. Springer, Berlin, pp. 125-154.

Supplement Section 2

Summary of key publications obtained for samples from the 2008 GEOTRACES expedition ANT XXIV/3 aboard the RV Polarstern.

Baars, O. and Croot, P.L., 2011. The speciation of dissolved zinc in the Atlantic sector of the Southern Ocean. Deep-Sea Res. II 58, 2720-2732.

Barré, N., Provost, C., Renault, A., Sennéchael, N., 2011. Fronts, meanders and eddies in Drake Passage during the ANT-XXIII/3 cruise in January February 2006: A satellite perspective. Deep-Sea Res. II 58, 2533-2554.

Behrendt, A., Fahrbach, E., Hoppema, M., Rohardt, G., Boebel, O., Klatt, O., Wisotzki, A., Witte, H., 2011. Variations of Winter Water properties and sea ice along the Greenwich meridian on decadal time scales. Deep-Sea Res. II 58, 2524-2532.

Bluhm, K., Croot, P.L., Huhn, O., Rohardt, G., Lochte, K., 2011. Distribution of iodide and iodate in the Atlantic sector of the southern ocean during austral summer. Deep-Sea Res. II 58, 2733-2748.

Croot, P.L., Baars, O., Streu, P., 2011. The distribution of dissolved zinc in the Atlantic sector of the Southern Ocean. Deep-Sea Res. II 58, 2707-2719.

Fahrbach, E., de Baar, H.J.W., Garcon, V.C., Provost, C., 2011. Introduction to physics, carbon dioxide, trace elements and isotopes in the Southern Ocean: The Polarstern expeditions ANT-XXIV/3 (2008) and ANT-XXIII/3 (2006). Deep-Sea Res. II 58, 2501-2508.

Fahrbach, E., Hoppema, M., Rohardt, G., Boebel, O., Klatt, O., Wisotzki, A., 2011. Warming of deep and abyssal water masses along the Greenwich meridian on decadal time scales: The Weddell gyre as a heat buffer. Deep-Sea Res. II 58, 2509-2523.

Klunder, M., Laan, P., Middag, R., De Baar, H., Van Ooijen, J., 2011. Dissolved iron in the Southern Ocean (Atlantic sector). Deep-Sea Res. II 58, 2678-2694.

Middag, R., de Baar, H.J.W., Laan, P., Cai, P.H., van Ooijen, J.C., 2011. Dissolved manganese in the Atlantic sector of the Southern Ocean. Deep-Sea Res. II 58, 2661-2677.

Middag, R., van Slooten, C., de Baar, H.J.W., Laan, P., 2011. Dissolved aluminium in the Southern Ocean. Deep-Sea Res. II 58, 2647-2660.

Middag, R., de Baar, H.J.W., Laan, P., Huhn, O., 2012. The effects of continental margins and water mass circulation on the distribution of dissolved aluminum and manganese in Drake Passage. J. Geophys. Res. C01019, doi:10.1029/2011JC007434.

Middag, R., de Baar, H.J.W., Klunder, M.B., Laan, P., 2013. Fluxes of dissolved aluminum and manganese to the Weddell Sea and indications for manganese co-limitation. Limnol.

Oceanogr. 58, 287-300.

Provost, C., Renault, A., Barré, N., Sennechael, N., Garcon, V., Sudre, J., Huhn, O., 2011. Two repeat crossings of Drake Passage in austral summer 2006: Short-term variations and evidence for considerable ventilation of intermediate and deep waters. Deep-Sea Res. II 58, 2555-2571.

Renault, A., Provost, C., Sennechael, N., Barré, N., Kartavtseff, A., 2011. Two full-depth velocity sections in the Drake Passage in 2006 – Transport estimates. Deep-Sea Res. II 58, 2572-2591.

Sudre, J., Garcon, V., Provost, C., Sennechael, N., Huhn, O., Lacombe, M., 2011. Short-term variations of deep water masses in Drake Passage revealed by a multiparametric analysis of the ANT-XXIII/3 bottle data. Deep-Sea Res. II 58, 2592-2612.

Thuróczy, C.E., Gerringa, L.J.A., Klunder, M.B., Laan, P., de Baar, H.J.W., 2011. Observation of consistent trends in the organic complexation of dissolved iron in the Atlantic sector of the Southern Ocean. Deep-Sea Res. II 58, 2695-2706.

Rutgers van der Loeff, M.R., Cai, P.H., Stimac, I., Bracher, A., Middag, R., Klunder, M.B., van Heuven, S.M.A.C., 2011. ^{234}Th in surface waters: Distribution of particle export flux across the Antarctic Circumpolar Current and in the Weddell Sea during the GEOTRACES expedition ZERO and DRAKE. Deep-Sea Res. II 58, 2749-2766.

van Heuven, S.M.A.C., Hoppema, M., Huhn, O., Slagter, H.A., de Baar, H.J.W., 2011. Direct observation of increasing CO2 in the Weddell Gyre along the Prime Meridian during 1973-2008. Deep-Sea Res. II 58, 2613-2635.

Venchiarutti, C., van der Loeff, M.R., Stimac, I., 2011. Scavenging of ^{231}Pa and thorium isotopes based on dissolved and size-fractionated particulate distributions at Drake Passage (ANTXXIV-3). Deep-Sea Res. II 58, 2767-2784.

Supplement Section 3

Material to support the interpretation that samples from the ACC and the Weddell Gyre feature two $\varepsilon^{114/110}$Cd vs. [Cd] trends with distinct slopes (see Abouchami et al., 2011).

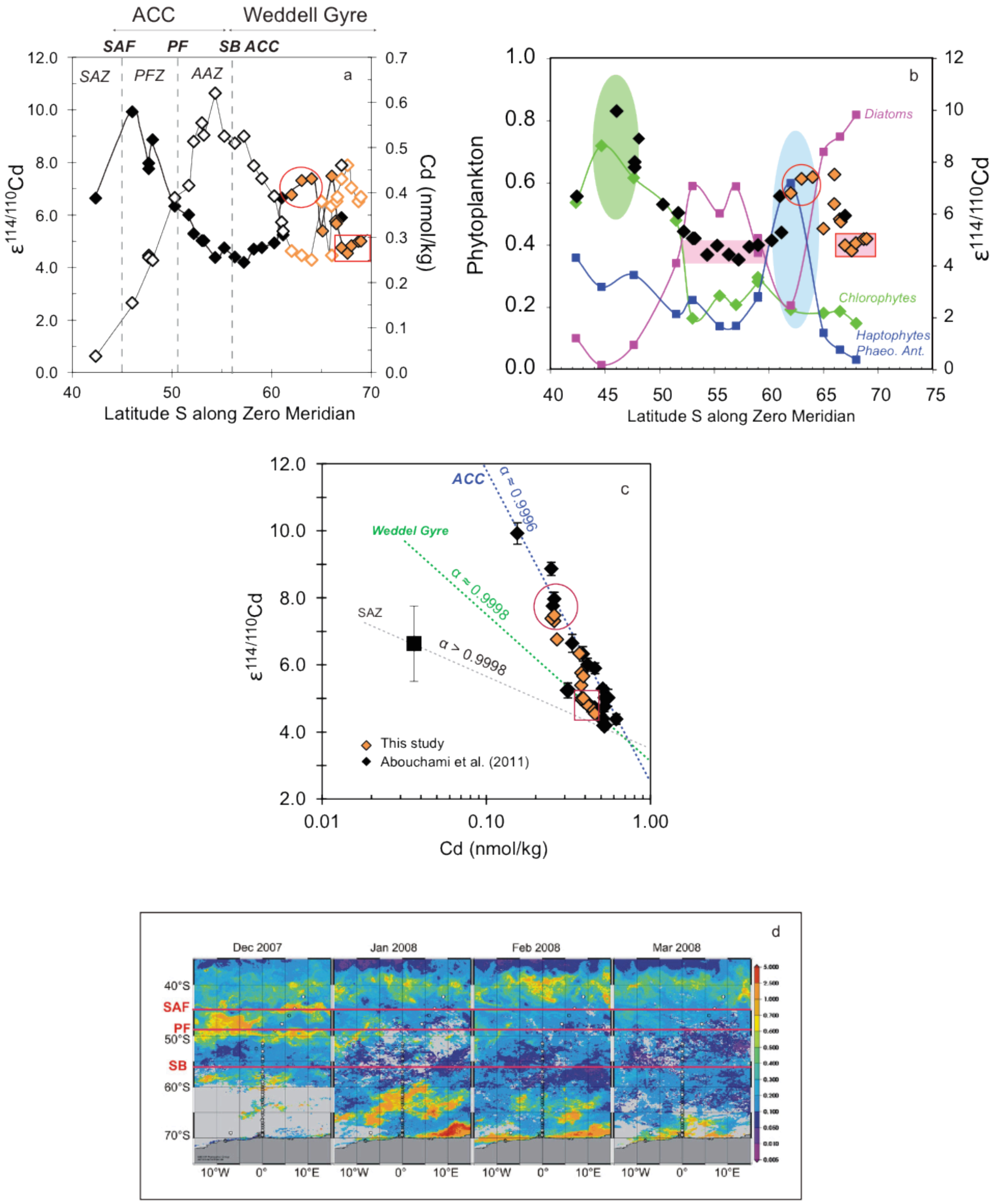

Figure S3.1: Summary of data for the Zero Meridian surface water transect in the Southern Ocean. Shown are (a) the new Cd and Cd isotope results of this study (orange symbols) and those from Abouchami et al. (2011) (blacks symbol) and (b) biological data (Alderkamp et al., 2011) as a function of latitude. These panels illustrate the relationship between the two Cd biogeochemical provinces of the ACC and Weddell Gyre and the Rayleigh fractionation lines shown in panel (c). Panel (d) summarizes monthly mean values for the satellite Chlorophyll-a distribution around the Zero Meridian section showing the progression of the phytoplankton bloom between December 2007 and March 2008 (taken from Rutgers van der Loeff et al., 2011).

Discussion of Fig. S3.1

The data circled in (a) to (c) correspond to the Weddell Gyre samples from 60-65°S which fall along the ACC line ($\alpha_{ACC} \approx 0.9996$) and feature the shift to heavier Cd isotope composition induced by the December 2007 phytoplankton bloom in this region. The red squares of panels (a) to (c) correspond to samples of this study from between 67-69°S that have Cd isotope signatures akin to the Weddell Gyre (samples 164 to 172; Table 1). These two groups match remarkably those identified on the basis of temperatures and major nutrient concentrations (see text). Samples from around 66°S, located in the southern branch of the Weddell Gyre, show contrasting changes in $\varepsilon^{114/110}$Cd and Cd concentration and as a result, plot between the two lines.

References

Abouchami, W., Galer, S.J.G., de Baar, H.J.W., Alderkamp, A.C., Middag, R., Laan, P., Feldmann, H., Andreae, M.O., 2011. Modulation of the Southern Ocean cadmium isotope signature by ocean circulation and primary productivity. Earth Planet. Sci. Lett. 305, 83-91.

Alderkamp, A.C., de Baar, H.J.W., Visser, R.J.W., Arrigo, K.R., 2010. Can photoinhibition control phytoplankton abundance in deeply mixed water columns of the Southern Ocean? Limnol. Oceanogr. 55, 1248-1264.

Rutgers van der Loeff, M.R., Cai, P.H., Stimac, I., Bracher, A., Middag, R., Klunder, M.B., van Heuven, S.M.A.C., 2011. ^{234}Th in surface waters: Distribution of particle export flux across the Antarctic Circumpolar Current and in the Weddell Sea during the GEOTRACES expedition ZERO and DRAKE. Deep-Sea Res. II 58, 2749-2766.

Supplement Section 4

Detailed statistical evaluation of the data for Southern Ocean surface water data from the Zero Meridian Transect and mixed layer samples from Stations 198, 245 and 249

Previously, Abouchami et al. (2011) concluded that their Southern Ocean samples define two distinct linear correlations in a plot of $\varepsilon^{114/110}$Cd vs. ln([Cd]), implying two distinct values of α. In detail, they found that the samples from ACC locations between 46°S and 56°S define a correlation with a slope equivalent to a fractionation factor of α_{ACC} = 0.99960, whilst most samples from 56°S to 61°S in the Weddell Gyre (WG) are in accord with a gentler trend indicative of α_{WG} = 0.99975 (Fig. 6a, main text). Abouchami et al. (2011) inferred that the Cd systematics of the samples are in accord with biological isotope fractionation in two regimes that are associated with distinct values of α, as a consequence of differences in phytoplankton biomass, community composition, and/or physiological mechanisms of Cd uptake (see Discussion in main text).

Using the combined dataset of this study and the investigation of Abouchami et al. (2011), it is possible to test if a 'two-trend' model fits the data significantly better than a simpler 'one-trend' model. As with any dataset, partitioning the data into smaller subsets and regressing each subset separately will result in a better fit than if regressing all data together. However, the improved fit to the data may not necessarily be statistically significant given the additional degree(s) of freedom and the reduced number of observations in each subset. This trade-off can be rigorously evaluated using a Likelihood Ratio Test (LRT; e.g., Neyman and Pearson, 1933).

Before testing, the data must be objectively partitioned into multiple sets. Using physical oceanographic data, it is reasonable to draw a partition along the boundary between the ACC and Weddell Gyre samples, equivalent to a 56 °S cutoff along the Zero Meridian. Samples from Stations 245 and 249, despite being from slightly south of the 56 °S cut-off, are outside of the Weddell Gyre, and are thus grouped with the ACC array (these samples also have similar Si* to the other ACC samples). Overall, this partition is consistent with the T, S, and nutrient data at the time of sample collection and follows from the two partitions used in Abouchami et al. (2011). Following partitioning, the log-likelihood for each model (i.e. one- or two-trends) was calculated using the sum of squares of residuals as the measure of the goodness-of-fit of each model (with the assumption that the residuals are normally distributed and have equal variance). The statistical significance of the improved fit of the two-trend over the one-trend model was then obtained by calculating the chi-square cumulative distribution at the result of the log-LRT with two degrees of freedom (corresponding to the difference in dimensionality between the one- and two-trend models).

Assuming closed system Rayleigh fractionation, our re-analysis confirms that the two-trend model fits the data significantly better than a single linear trend ($p = 1 \times 10^{-7}$; Fig. S4.1). This result is in accord with the findings of Abouchami et al. (2011). However, the slopes (i.e., the apparent α values) of the two trends are identical ($\alpha_{ACC} = 0.99959 \pm 0.00005$; $\alpha_{WG} = 0.99959 \pm 0.00009$) with a slight offset between the regressions of 1.1 ε (Fig. S4.1). Furthermore, the slopes of the two regression lines are also identical to the one-trend slope of $\alpha = 0.99959 \pm 0.00008$ (all uncertainties quoted as ±2sd; with n = 15, 22, and 37, respectively). This result suggests that Cd uptake from Southern Ocean seawater may be governed by only a single fractionation factor of $\alpha \approx 0.9996$.

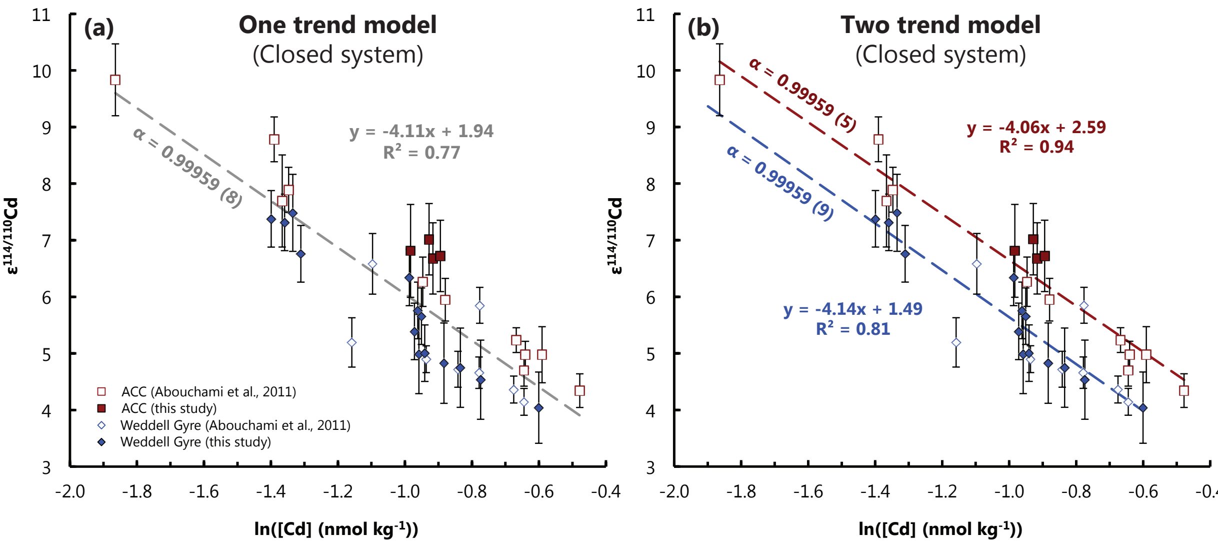

Fig. S4.1 Comparison of one vs. two-trend models for closed system Rayleigh fractionation. The data have been partitioned into two groups corresponding to their oceanography. The two panels illustrate the partitioning for the (a) one and (b) two-trend models, respectively. The numbers in brackets denote the uncertainty on the fractionation factor (±2sd).

If assuming open system fractionation, the fit of a two-line model is also significantly improved on the one-line model ($p = 9 \times 10^{-9}$; Fig. S4.2). As with the closed-system model, the slopes (m) of the two separate regression lines are within uncertainty of one-another ($m_{ACC} = -11.7 \pm 1.5$; $m_{WG} = -11.0 \pm 2.6$; ±2sd, n = 15 and 22, respectively), as well as being within uncertainty of the single regression slope of $m = -11.1 \pm 2.4$ (±2sd, n = 37). In this case, no assumptions are made with regards to starting water compositions or the extent of Cd utilization. As such, slopes are reported 'as is' and are not converted to fractionation factors. A slight offset between separate regression lines, as seen in the closed system model, is also seen in the open-system case, equivalent to 1.4 ε (Fig. S4.2).

The offset between the two trends may be evidence of the different water mass histories, despite the common source water for both regions (Circumpolar Deep Water, CDW). That the waters north of 56 °S are ~1 ε-unit 'heavier' than more southern waters could be due to a number of reasons. The difference may be caused by more extensive Cd removal from CDW prior to its northward advection (i.e., waters north of the APF have an isotopically 'heavier' starting point), or may be attributed to additional inputs of Cd into the more northern waters as they traverse along the flowpath (e.g., vertical mixing of heavier Atlantic-sourced deep waters).

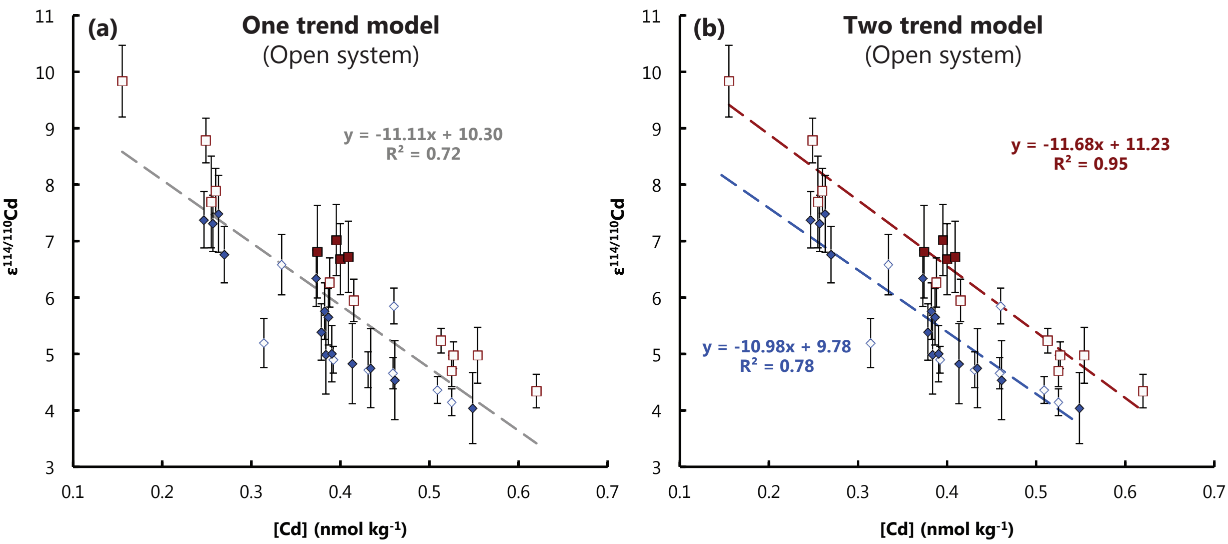

Fig. S4.2 Comparison of one vs. two trend models for open-system Rayleigh fractionation. T data have been partitioned into two groups corresponding to their oceanography. The two panels illustrate the partitioning for the (a) one and (b) two-trend models, respectively.

References

Abouchami, W., Galer, S.J.G., de Baar, H.J.W., Alderkamp, A.C., Middag, R., Laan, P., Feldmann, H., Andreae, M.O., 2011. Modulation of the Southern Ocean cadmium isotope signature by ocean circulation and primary productivity. Earth Planet. Sci. Lett. 305, 83-91.

Neyman, J., and E. S. Pearson (1933). On the problem of the most efficient tests of statistical hypotheses, Phil. Trans. R. Soc. Lond. A 231, 289–337.

Supplement Section 5

Published Cd isotope data for global open-ocean deep waters (≥ 1 km depth)

Cruise	Ocean Basin/Region	Date of sampling	Station/Sample	Water depth	Lat.	Long.	[Cd]	2sd	ε114/110Cd rel to NIST 3108 Cd	2sd	ε114/110Cd rel to Alfa Cd Zurich	2sd	ε114/110Cd rel to JMC Cd Münster	2sd	Reference
Units / Offset from NIST 3108 Cd				m			nmol/kg				-0.20		-0.89		1
AWS 2000	Arctic Ocean	24/8/00	3	3000	75.20	-149.90	0.204	0.000	*4.16*	1.00	4.36	1.00			2
GEOTRACES Atlantic Intercal	Atlantic/BATS B	22/6/08	21 Geotraces 2679	1000	31.77	-64.08	0.294		5.55	0.56					3
GEOTRACES Atlantic Intercal	Atlantic/BATS B	22/6/08	GDI 49+50+51	2000	31.77	-64.08	0.271	0.002	4.84	0.67					3
GEOTRACES Atlantic Intercal	Atlantic/BATS B	22/6/08	9 Geotraces 2674	2500	31.77	-64.08	0.293		4.16	0.56					3
GEOTRACES Atlantic Intercal	Atlantic/BATS B	22/6/08	4 Geotraces 2672	3500	31.77	-64.08	0.295		4.49	0.56					3
Endeavor 408	N-Atlantic	12/7/05	2	2900	33.00	-72.00	0.281	0.000	*2.90*	0.77	3.10	0.77			2
ANT24-3 IPY-GEOTRACES 2008	Southern Ocean	21/3/08	198	1000	-65.61	-36.40	0.815		2.56	0.26					4
ANT24-3 IPY-GEOTRACES 2008	Southern Ocean	21/3/08	198	2000	-65.61	-36.40	0.788		2.30	0.35					4
ANT24-3 IPY-GEOTRACES 2008	Southern Ocean	21/3/08	198	3000	-65.61	-36.40	0.776		2.94	0.65					4
ANT24-3 IPY-GEOTRACES 2008	Southern Ocean	21/3/08	198	4000	-65.61	-36.40	0.762		2.55	0.65					4
ANT24-3 IPY-GEOTRACES 2008	Southern Ocean	21/3/08	198	4702	-65.61	-36.40	0.754		1.69	0.65					4
ANT24-3 IPY-GEOTRACES 2008	Southern Ocean	27/3/08	216	1000	-63.70	-50.84	0.783		2.23	0.49					4
ANT24-3 IPY-GEOTRACES 2008	Southern Ocean	27/3/08	216	1500	-63.70	-50.84	0.782		2.49	0.76					4
ANT24-3 IPY-GEOTRACES 2008	Southern Ocean	27/3/08	216	2000	-63.70	-50.84	0.771		1.93	0.76					4
ANT24-3 IPY-GEOTRACES 2008	Southern Ocean	27/3/08	216	2450	-63.70	-50.84	0.737		2.99	0.33					4
ANT24-3 IPY-GEOTRACES 2008	Southern Ocean	10/4/08	249	1250	-56.12	-63.76	0.807		2.46	0.35					4
ANT24-3 IPY-GEOTRACES 2008	Southern Ocean	10/4/08	249	1750	-56.12	-63.76	0.761		2.81	0.58					4
ANT24-3 IPY-GEOTRACES 2008	Southern Ocean	10/4/08	249	2500	-56.12	-63.76	0.744		2.40	0.58					4
ANT24-3 IPY-GEOTRACES 2008	Southern Ocean	10/4/08	249	3000	-56.12	-63.76	0.759		2.71	0.58					4
ANT24-3 IPY-GEOTRACES 2008	Southern Ocean	10/4/08	249	4000	-56.12	-63.76	0.763		2.50	0.58					4
ANT24-3 IPY-GEOTRACES 2008	Southern Ocean	10/4/08	249	4253	-56.12	-63.76	0.767		2.83	0.58					4
ANT XX/2	Southern Ocean	10/1/03	63/131-1	4000	-61.00	23.00	0.815	0.001	*2.71*	1.00	2.91	1.00			2
SAFe	N Pacific		SAFe D1	1000	30.00	-140.00	1.012	0.003	*3.31*	0.11			4.20	0.11	5
IOC 2002	N-Pacific	22/5/02	7	1200	24.30	170.30	0.994	0.001	*3.02*	1.03	3.22	1.03			2
IOC 2002	N-Pacific	22/5/02	7	4000	24.30	170.30	0.862	0.000	*2.78*	1.00	2.98	1.00			2
IOC 2002	N-Pacific	22/5/02	7	5700	24.30	170.30	0.834	0.002	*3.03*	1.56	3.23	1.56			2
IOC 2002	N-Pacific	30/5/02	9	1200	22.80	-158.00	0.988	0.000	*2.69*	1.20	2.89	1.20			2

Averages based on dataset	Number of samples (n)	[Cd] nmol/kg	±2sd [Cd]	±2se [Cd]	ε114/110Cd rel to NIST 3108 Cd	±2sd εCd	±2se εCd
Global deep water	27	0.693	0.472	0.091	3.00	1.75	0.34
Deep water from Southern & Pacific Ocean	21	0.813	0.162	0.035	2.62	0.74	0.16
Southern Ocean deep water	16	0.774	0.045	0.011	2.51	0.68	0.17
Southern Ocean samples of this study	15	0.771	0.041	0.011	2.49	0.69	0.18

Isotopic data in italics were recalculated based on the isotopic offsets between the reference materials given above.
References. 1: Abouchami et al., 2012. 2: Ripperger et al., 2007; 3: Boyle et al., 2012. 4: This study. 5: Xue et al., 2012.
The deep water Cd isotope data of Yang et al. are not compiled here because the South China Sea is a restricted ocean basin

Supplement Section 6

Calculations applied to estimate the Cd content and C/Cd ratio of plankton, as applied to model remineralization

Phytoplankton composition following Ho et al. (2003)

Composition of (dry) plankton tissue is $(C_{124}\ N_{16}\ P_1\ S_{1.3}\ K_{1.7}\ Mg_{0.56}\ Ca_{0.5})_{1000}\ Sr_{5.0}\ Fe_{7.5}\ Zn_{0.80}\ Cu_{0.38}\ Co_{0.19}\ Cd_{0.21}\ Mo_{0.03}$

This is equivalent to ~1850 g per mol P. Hereby, the best estimate of the Cd quota (relative to 1 mol P) is 0.21 mmol but the quota can reasonably vary from 0.05 to 0.5 mmol Cd

Best estimate Cd quota yields [Cd] = 1.1×10^5 nmol/kg and molar C/Cd = 5.9×10^5

Diatom composition following Price (2005) and Ho et al. (2003)

Composition of (dry) HNLC diatoms (with Cd quota of Ho et al., 2003) is $(C_{70}\ N_{10}\ Si_{5.9}\ P_1\ Fe_{0.00074})_{1000}\ Cd_{0.21}$

Assuming that Si does not dissolve during remineralization of tissue in upper water column, the remineralized part of diatoms is equivalent to ~840 g per mol P

Assuming best estimate Cd quota relative to P is appropriate for diatoms, the composition yields [Cd] = 2.3×10^5 nmol/kg and molar C/Cd = 3.3×10^5

Wet versus dry plankton weight

In water, plankton contain a sizeable component of 'body water', which is considered to be part of the 'system' during remineralization. The studies of Beers (1966) and Omori (1969) indicate that dry to wet plankton mass ratios typically vary between 3 and 30%, with most results between 5 and 20%.

Based on this, 'total wet plankton' are estimated to have a Cd concentration that is about 10x lower compared to the Cd content estimated above for dry plankton tissue.

Summary

The results validate the use of the following parameters for remineralized biomass in the manuscript (see section 5.3.2 and Fig. 7a):

[Cd] = 2.0×10^4 nmol/kg

Molar C/Cd = 3.3×10^5

References

Beers, J.R., 1966. Studies on the chemical composition of the major zooplankton groups in the Sargasso Sea off Bermuda. Limnol. Oceanogr. 11, 520-528.

Omori, M., 1966. Weight and chemical composition of some important oceanic zooplankton in the North Pacific Ocean. Mar. Biol. 3, 4-10.

Price, N.M., 2005. The elemental stoichiometry and composition of an iron-limited diatom. Limnol. Oceanogr. 50, 1159-1171.

Ho, T.-Y., Quigg, A., Finkel, Z.V., Milligan, A.J., Wyman, K., Falkowski, P.G., Morel, F.M.M., 2003. The elemental composition of some marine phytoplankton. J. Phycol. 39, 1145-1159.